Solar Energy Materials & Solar Cells xxx (xxxx) xxx

Contents lists available at ScienceDirect

Solar Energy Materials and Solar Cells

journal homepage: http://www.elsevier.com/locate/solmat

Kinetics of degradation-induced photoluminescence in ethylene-vinyl-acetate as used in photovoltaic modules

Ronald Steffen [a,*], Mohammed Abdul-Hamza Akraa [a,b], Beate Röder [a]

[a] Humboldt-Universität zu Berlin, Department of Physics, Newtonstraße 15, 12489, Berlin, Germany
[b] University of Babylon, College of Material's Engineering, Dept. of Eng. of Polymers and Petrochemical Industries, Iraq

ARTICLE INFO

Keywords:
Degradation-induced polymer photoluminescence
Solid-state photoluminescence
Polymer thermal degradation
Ageing characterization
Ethylene vinyl acetate

ABSTRACT

The degradation-induced polymer photoluminescence and absorbance spectra of two differently stabilized commercial EVA grades are investigated under conditions of exposure to dry heat at 85 °C, 115 °C and 135 °C and moisture of 85% relative humidity at 85 °C. In addition to the photoluminescence signal as described before, new features are identified for both, absorbance and photoluminescence spectra. Most prominently, the formerly suggested initial luminescence signal of the model of degradation-induced polymer photoluminescence is identified at an emission wavelength of about 310 nm. It is shown to exhibit a sequential reaction kinetics and to be related to the absorbance of carbonyl sates at 285 nm. The kinetic parameters of these signals are quantitatively evaluated and discussed in the scope chemical degradation and physical relaxation processes. We demonstrate that additive formulations can be distinguished by means of degradation-induced polymer photoluminescence, enabling its application for the characterization and optimization of polymeric materials.

1. Introduction

Polymeric materials are used as front or back sheet encapsulating material in photovoltaic modules. They provide mechanical stability, optical coupling, electrical isolation and protection against environmental conditions [1]. Throughout their operational lifetime the encapsulating polymeric materials have to withstand a variety of climate conditions depending on the geographical region the photovoltaic module is installed in Ref. [2]. Therefore, characterization and optimization of the outdoor performance and degradation of photovoltaic modules is important [3] to fulfill customer's expectations on service life of more than 25 years. To this end, polymeric materials are optimized to withstand specific types of exposure conditions like high temperatures or exposure to UV radiation or humidity.

However, sooner or later the polymeric material will start to degrade altering its optical and mechanical properties, and thereby reducing the overall performance of the photovoltaic device. This degradation can particularly effect new technologies based on polymeric materials as employed in organic photovoltaic or solar-thermal devices [4–6]. Determination of the degradation state and prediction of the lifetime of polymeric materials under different exposure conditions are therefore important topics [7–9].

Because of its physical-chemical properties and its low cost ethylene vinyl acetate (EVA) is, with nearly 80% market-share, the most commonly used embedding material in photovoltaic devices [1]. With respect to the maximum service life of photovoltaic modules, corrosion and delamination have been identified as the main failure modes related to the degradation of the encapsulation material EVA [1]. In addition, EVA is known to undergo discoloration under different exposure conditions [10–12]. Although discoloration has no significant effect on power generation in a PV-module [1,13], it is an indicator of chemical degradation, a process which eventually involves the generation of acetic acid leading to the above mentioned failure modes [1].

To measure the degradation state of polymeric materials, a number of laboratory-based methods are available like thermal gravimetric analysis, thermal differential analysis, differential scanning calorimetry [14–16] or (for photovoltaic modules) thermally stimulated current technique [17]. Also optical methods like Raman and FTIR are frequently used [11,18]. However, all the above methods require sampling of EVA material from the photovoltaic device, are technically more complex than luminescence methods and cannot be applied in the field.

Already in the 1960s it was suggested that polymer

Abbreviations: TTS, time-temperature-superposition; EVA, ethylene vinyl acetate; DIPL, degradation-induced polymer photoluminescence; r.h., relative humidity; DOS, density of states.

* Corresponding author.
E-mail address: rsteffen@physik.hu-berlin.de (R. Steffen).

https://doi.org/10.1016/j.solmat.2019.110294
Received 1 April 2019; Received in revised form 22 July 2019; Accepted 11 November 2019

photoluminescence could be used to monitor the degradation state of polymeric materials [19–22], and also EVA was investigated thoroughly [10,23,24]. However, due to the lack of a quantitative understanding of the method, it did not gain widespread acceptance. Over the last years our group was able to put this method on a quantitative basis by developing a model to describe the degradation-induced polymer photoluminescence (DIPL) [25]. We also demonstrated its application for the determination of apparent activation energies of the degradation process of different polymeric materials [26,27], which is an important parameter required for polymer lifetime prediction [11,12]. The photoluminescence method has the advantage of being non-destructive and, from the technical point of view easy to be applied in the field, which was demonstrated already in a number of publications [28,29]. In addition, a correlation could be established between the thermal properties of degraded EVA and its photoluminescence [28] and degree of cross-linking [29–31], respectively.

The discoloration of EVA was also shown to depend on diffusion processes of oxygen and water occurring inside photovoltaic modules leading to diffusion-limited oxidation processes [9]. Gagliardi et al. [32] suggested a computational reaction-diffusion model to predict degradation kinetics and discoloration of EVA and found values of 65 kJ/mol and ca. 106 kJ/mol for the activation energies of degradation reactions and 39 kJ/mol for the activation energy of the diffusion of water to be consistent with their experimental results. Significantly higher activation energies between 162 and 176 kJ/mol have been reported for weight loss reactions of EVA at $T > 300\,^{\circ}C$ as determined by thermal gravimetric analysis or differential scanning calorimetry [33,34].

Here we investigate the degradation of two commercially available grades of EVA under dry heat and damp heat conditions by means of degradation-induced polymer photoluminescence to estimate the apparent activation energies of the degradation process.

2. Material and methods

2.1. Sample material and ageing

Two different cured grades of EVA employed as either front-sheet or back-sheet material, here labeled EVA grade A and EVA grade B, of unknown additive composition as used in commercial photovoltaic modules, have been exposed to dry heat conditions of 85 °C, 115 °C and 135 °C and damp heat of 85% r.h. at 85 °C. EVA samples of about 3×3 cm size were cut from bigger EVA sheets and were used as provided by the manufacturer.

2.2. Absorbance measurements

Absorbance measurements were conducted on a Shimadzu UV-2450 spectrometer with a spectral bandwidth of 1 nm.

2.3. Photoluminescence measurements

Photoluminescence measurements were conducted on a Jasco FP-8500 fluorescence spectrometer equipped with internal second order filters and employing a solid state sample holder titled by 30° with respect to the incident excitation beam. Due to the weak nature of polymer photoluminescence and the peculiarities of measuring photoluminescence from transparent solid-state samples, additional measures had to be taken to avoid distortion of the spectra by scattered excitation and/or stray light omnipresent in all monochromator based systems. To this end, two different approaches have been used. For measurements with fixed excitation wavelength appropriate cut-off filters (Semrock FF01-280-10/BLP01-325R) have been employed. For measurements of excitation-emission maps, polarizers were used in perpendicular

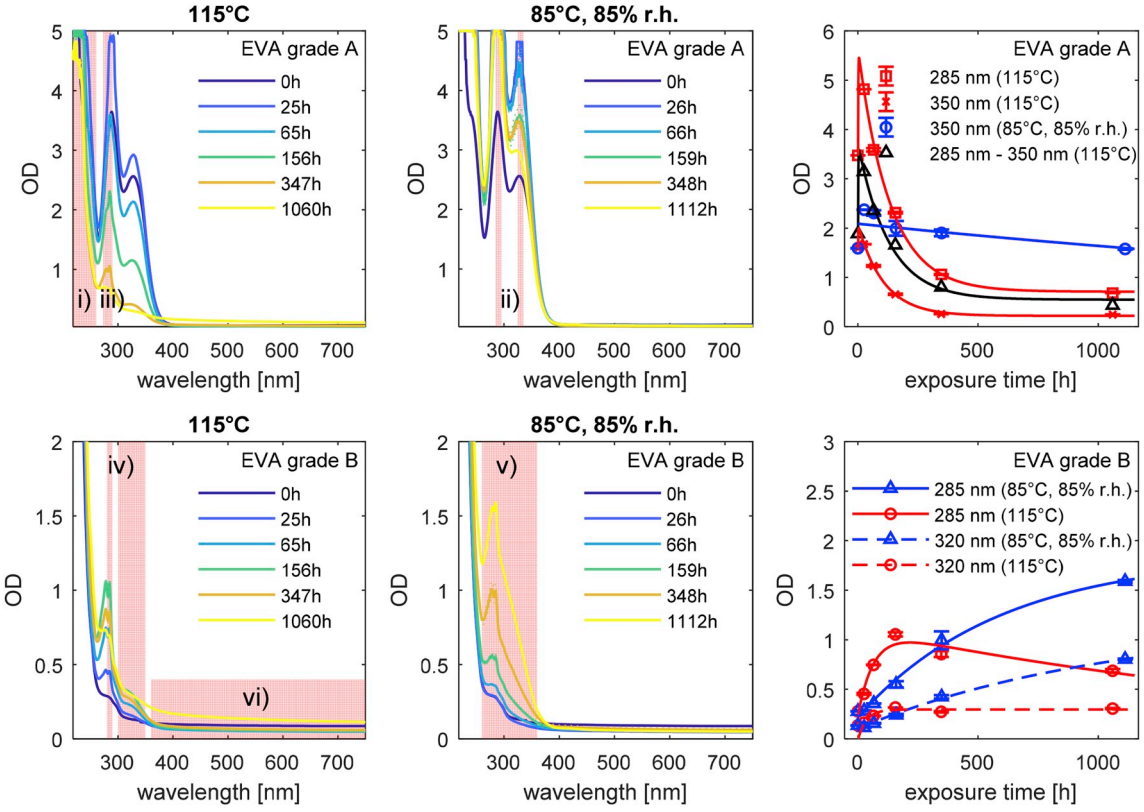

Fig. 1. Absorbance spectra (left and middle column) and kinetics (right column) of EVA grades A (top row) and B (bottom row) in dependence of exposure time for different exposure conditions and exposure times as stated in the figure. Kinetics are depicted for EVA grade A: features ii) at 350 nm (due to the distortion of the signal at 330 nm) and iii) at 285 nm; and EVA grade B features iii) at 285 nm and iv) and v) at 320 nm.

configuration to provide a better contrast ratio between photoluminescence and stray light. The latter approach is based on the fact that scattered light and stray light are usually highly polarized whereas the polymer photoluminescence signal was found to be largely depolarized (see also [25]).

All spectra shown in this paper were spectrally corrected by employing Rhodamine B and HITCI as quantum counters.

To account for lateral inhomogeneities within samples, for measurements at fixed excitation wavelengths, mean values, and standard deviations were calculated from four different rotational positions of any individual sample (two for each face).

2.4. Data analysis methods

All data analysis was performed in Matlab employing linear or nonlinear regression. For measurements where standard deviations were available robust (bi-square weights) weighted least-squares were used with weights calculated as $1/\sigma^2$.

For time-temperature-superposition analysis a_T-values were determined by employing the Matlab fmincon function minimizing $1-R^2_{adjusted}$ of a global nonlinear least-square fit over all temperatures to an appropriately selected model function. Model functions were either exponential, polynomial or power law functions.

3. Results

3.1. Absorbance measurements

Fig. 1 shows the absorbance spectra and extracted absorbance kinetics of the investigated EVA grades under dry heat exposure of 115 °C and damp heat exposure of 85 °C/85% (r.h.). Altogether, depending on EVA grade and exposure condition, we can identify six different absorbance features:

i) intrinsic absorbance of EVA <260 nm
ii) absorbance of an UV-absorbing additive (maxima at 290 and 330 nm),
iii) absorbance of carbonyl species (maxima at 278 and 285 nm),
iv) absorbance bands at 285 and between 300 and 350 nm (most apparent for unaged samples), and
v) a broad absorbance band (260–360 nm)
vi) an absorbance tail extending to above 800 nm (discoloration)

The intrinsic absorbance i) of the EVA backbone below 260 nm can be observed under all conditions. The OD values of this absorbance exceed the dynamic range of OD 5 of the employed spectrometer and this absorbance is not further evaluated.

Occurrence of the other absorbance features depends on EVA grade and exposure condition. The 0 h reference sample of EVA grade A (top row) is characterized by absorbance bands with maxima around 290 nm and 330 nm (feature ii)), which is consistent with the benzophenone-based UV-absorbing additive Cyasorb 531. The 0 h reference sample of EVA grade B (bottom row) only exhibits minor absorbance features around 285 nm and 300–350 nm (feature iv)). This indicates two different additive formulations for the two investigated EVA grades.

Under dry heat conditions at 115 °C the absorbance of the UV-absorbing additive of EVA grade A (feature ii)) disappears with a lifetime of $\tau \approx 130$ h (Table 1) and is replaced by a much narrower absorbance band with peaks at 278 and 285 nm (feature iii)). This feature accounts for most of the fast initial rise of the signal as can be seen by subtracting the signal at 350 nm (black solid line). Absorbance features of this kind are consistent with n -> π* transitions of carbonyls[1] [35] and are well-known to occur due to the oxidative degradation of different polymers [36,37].

Table 1
Time-constants for absorbance kinetics at 350 nm under 115 °C dry heat exposure estimated from a bi-exponential model.

	τ_{rise}	τ_{decay}
EVA grade A	0.8 h	130 h
EVA grade B	64 h	2078 h

An additional band (feature iv)) is observed between 300 and 350 nm. The absorbance features iii) and iv) can also be identified for EVA grade B. It should be noted that, in contrast to feature ii), the absorbance of feature iii) first increase and then decrease again for very long exposure times. This is more obvious from comparison of the kinetics (solid red lines in Fig. 1, right) at 350 nm (EVA grade A) and 285 nm (EVA grade B). In contrast, the absorbance at 320 nm, representing feature iv), exhibits a saturating behavior.

The sample of EVA grade B exposed for 1060 h at 115 °C dry heat exhibits an additional absorbance tail (feature vi)) which extends to above 800 nm. This type of absorbance can be readily assigned to discoloration of the sample as will be detailed in the discussion.

Under damp heat conditions at 85 °C/85% r.h. for EVA grade A the absorbance as related to feature ii) is observed to decrease by about one-third of its original amplitude ($\tau \approx 4100$ h). No other absorbance features can be observed in this case because they are superimposed on the absorbance of the UV-absorbing additive (feature ii)). For EVA grade B in addition to the absorbance observed under dry heat conditions a broad absorbance between 260 and 360 nm (feature v)) is observed. This absorbance is probably related to moisture or wetting of the sample. It should be noted that subsequent drying of samples did not remove this signal, indicating that this signal is related to an irreversible chemical modification.

It should be pointed out that the absorbance spectrum of EVA grade A after 1060 h of dry heat exposure is comparable to the 0 h reference sample of EVA grade B. This indicates the complete consumption of the UV-absorbing additive and also the disappearance of the carbonyl related absorbance feature iii). For EVA grade B feature iii) significantly decreased, but did not completely disappear at this time scale (compare kinetics, solid red line).

3.2. Degradation-induced polymer photoluminescence

The photoluminescence spectra excited at 280 nm for both exposure conditions are shown in Fig. 2 for one series of samples. Phenomenologically, for both EVA grades the same photoluminescence features can be identified. For dry heat exposure the photoluminescence is characterized by two bands. One broad emission between ca. 350–650 nm which increases with prolonged exposure and which is consistent with the long-wavelength photoluminescence (or density of states photoluminescence, DOS-photoluminescence) as discussed before [25]. The second photoluminescence feature can be identified at wavelength shorter than 350 nm. It is steeply increasing towards shorter wavelength and in these measurements cut-off by the employed filters.

The latter band can also be found under damp heat exposure (Fig. 2, right). In addition, a new photoluminescence feature exhibiting two bands centered around 381 and 397 nm is found. This photoluminescence was not observed under any other conditions and seems to be characteristic for damp heat exposure.

The kinetics of the photoluminescence signals under dry heat exposure (Fig. 3) for the two identified photoluminescence bands, i.e. the long-wavelength (DOS) photoluminescence (450–750 nm, Fig. 3, bottom) and the short-wavelength band (320–380 nm, Fig. 3, top) exhibit characteristically different kinetic behavior. Whereas the DOS-

[1] Compare e.g.: acetone 265 nm, 2-undecanone 280 nm, cyclohexanone 280 nm, 3-methyl-2-butanone 280 nm, phenol 270, 285 nm, 4-methyl-2-penten-2-one 240, 315, 280 nm, methyl vinyl ketone 320, 280 nm.

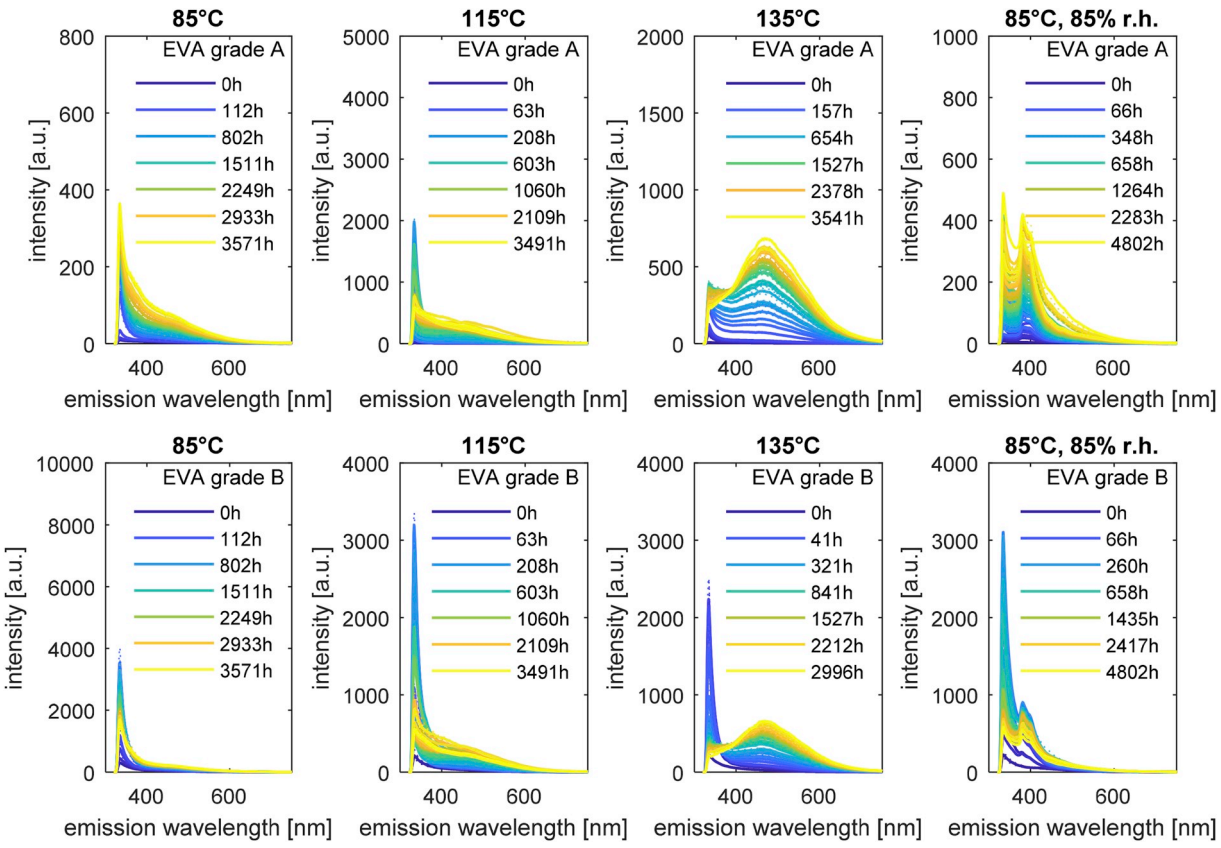

Fig. 2. Photoluminescence spectra of EVA grade A (top row) and EVA grade B (bottom row) at 280 nm excitation under different exposure conditions and exposure times as stated in the figure. Dotted lines indicate the standard deviation of four averaged spectra. For this measurement cut-off filters where used to suppress scattering artifacts.

photoluminescence exhibits a slow power-law rise as usually observed also for other polymeric materials in the early stages of degradation [26,27,38], the short-wavelength photoluminescence signal below 350 nm exhibits a rapid increase with a subsequent decay, which is indicative of a sequential process. This sequential kinetics is more pronounced for EVA grade B and is superimposed on the DOS-photoluminescence as is most apparent for the temperature of 135 °C where the DOS-photoluminescence decreases again for long exposure times due to a bathochromic shift of this photoluminescence band (compare [26]).

Comparing the short-wavelength photoluminescence kinetics to the 285 nm absorbance kinetics above (Fig. 1), it can be seen that for both EVA grades the kinetics match on a qualitative basis. For EVA grade A absorbance and short-wavelength photoluminescence kinetics rise and decay faster as for EVA grade B. This suggests that the short-wavelength photoluminescence signal can be attributed to the 285 nm absorbance feature, which is related to the absorbance of carbonyls. This short-wavelength signal is phenomenologically consistent with the initial photoluminescence of the DIPL-model as described in Ref. [25].

For exposure to 85% r.h. at 85 °C, despite of the additional photoluminescence signal, the kinetics are comparable to those of 85 °C dry heat exposure. Therefore, this kinetics will not be discussed here in more detail.

3.2.1. *Lateral inhomogeneity*

One of the most important questions about the application of EVA in the solar panel industry is the homogeneous distribution of additives within the EVA raw material. This influences, e.g. the lamination process. To test for this large-scale lateral inhomogeneity, for both EVA grades a sequence of four samples, evenly distributed over one row of a 50 cm sheet of EVA, was taken and the full measurement series of at least 3000 h exposure was repeated four times. Because of these extensive exposure times, these experiments could be conducted for one temperature, i.e. 115 °C, only.

We found that, although the precision of the individual photoluminescence measurements as estimated from the error bars (standard deviation of four measurements) is reasonably good, subsequent runs on different samples under identical conditions were not always reproducible as is illustrated in Fig. 3. For both grades the four independent runs on independent samples exhibit distinctly different kinetic behavior in the short-wavelength region. For the DOS-photoluminescence a deviation from power-law behavior was found for longer exposure times.

For the short-wavelength photoluminescence two kinetic patterns identical to those observed for either 85 °C or 135 °C were observed. For grade A, two samples exhibited a power law kinetic shape comparable to the other two temperatures or the DOS-photoluminescence signal. The other two samples exhibited a sequential kinetic shape (superimposed on the power-law kinetics).

For grade B, two samples showed a fast rise followed by a fast decay superimposed on a power law kinetics comparable to the pattern observed for 135 °C. The other two exhibit a fast rise followed by a slower decay as is also observed for 85 °C.

Since the precision of the measurements is reasonably good, and this experiment showed that kinetics of the two identified types can be measured reproducibly, we attribute the observance of two different types of kinetics to a lateral inhomogeneity of the additive distribution within the EVA sheet.

Summarizing the above discussion, we were able to identify two spectrally and kinetically separable photoluminescence bands, i.e. a short-wavelength band exhibiting a sequential kinetics which we attribute to the direct photoluminescence from carbonyl-related states and which we identified with the initial photoluminescence signal as

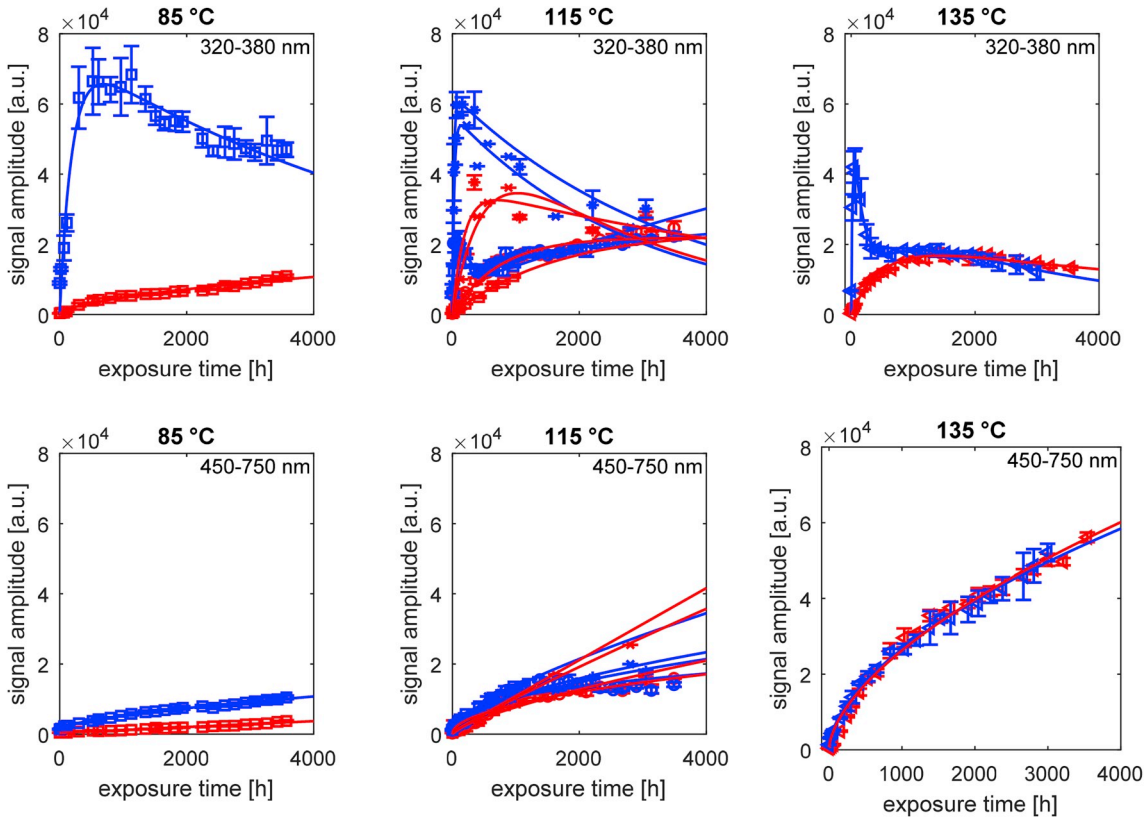

Fig. 3. Integrated photoluminescence kinetics under dry heat exposure., EVA grade A (red) and EVA grade B (blue). Upper: 320–380 nm, lower: 450–750 nm. For 115 °C four runs with independent samples are shown (compare text). For this measurement cut-off filters where used to suppress scattering artifacts. (For interpretation of the references to color in this figure legend, the reader is referred to the Web version of this article.)

proposed in Ref. [25], and a long-wavelength (DOS-photoluminescence) band which can be identified as the DOS-photoluminescence as described before [25].

3.2.2. Initial photoluminescence

Because in the measurement of Fig. 2 the short-wavelength band, which we identified with the proposed initial photoluminescence signal, was cut-off by the applied filter (which was required to suppress scattering artifacts), we repeated the measurement at 115 °C dry heat on an independent set of samples employing polarizers instead of filters to be able to resolve the full short-wavelength band (Fig. 4). Here we analyze in more detail the photoluminescence spectra and kinetics of one individual sample. Despite the above mentioned inhomogeneity this will give more insight into the physical processes determining the photoluminescence signal.

It can be seen that although the spectra for both EVA grades under all conditions are qualitatively comparable, the relative contribution of the carbonyl (initial photoluminescence) signal is significantly larger for EVA grade B. This is most striking for 85 °C dry heat, where for EVA grade A at about 2000 h of exposure the carbonyl signal exhibits only twice the amplitude of the DOS-photoluminescence signal, whereas for EVA grade B the ratio is greater than 2000.

This indicates different reaction rates of carbonyl formation and is a consequence of the sensitivity of the degradation-induced polymer photoluminescence (DIPL) kinetics to the additive formulation. For EVA grade A, the degradation process (increase of carbonyl photoluminescence) is much slower than for EVA grade B, which presumably is related to the difference in additive formulation for both EVA grades. We now attempt to quantify the kinetics of both photoluminescence signals by the model-free approach of time-temperature superposition (TTS) and subsequently by a simple model-testing approach.

3.2.3. Model-free analysis of DOS-DIPL by time-temperature-superposition

Analysis of the DOS-photoluminescence kinetics by time-temperature-superposition (TTS) provides a model-free estimation of the apparent activation energy (E_a) of the degradation process [39]. The TTS-analysis is shown in Fig. 5 for the measurement series employing filters (compare Fig. 3). Because of the afore-mentioned deviation of the kinetics at 115 °C, this data was not included in TTS-analysis. Instead the shift-factor for 115 °C was calculated from the 85 °C and 135 °C data based on an Arrhenius relationship. Nevertheless, the 115 °C data reasonably well superimposes on the data for the other two temperatures, indicating the validity of the Arrhenius approach. For EVA grade A E_a is estimated to be about 92 kJ/mol and for EVA grade B 74 kJ/mol (see Fig. 6).

The deviation from power-law behavior as mentioned before is also apparent in the TTS-plots. As already mentioned above this can be attributed to a lateral equilibration process of the distribution of additives and/or degradation products. This hypothesis is supported by the fact that a sufficient overlap within the TTS-plot is provided by the 85 °C and 135 °C kinetics already, for which a local homogeneity of the additive distribution of the mobile phase of additives is anticipated. The first 600 h of the 115 °C kinetics nevertheless reasonably well superimpose on the other two kinetics traces.

For measurements employing polarizers instead of filters TTS-analysis yields E_a-values of 114 kJ/mol for EVA grade A (Fig. 6) and 23 kJ/mol for EVA grade B (Fig. 7). This is qualitatively $(E_a(EVA\ grade\ A) > E_a(EVA\ grade\ B))$ consistent with the values estimated from the measurements employing filters as discussed above, but differs significantly on a quantitative level.

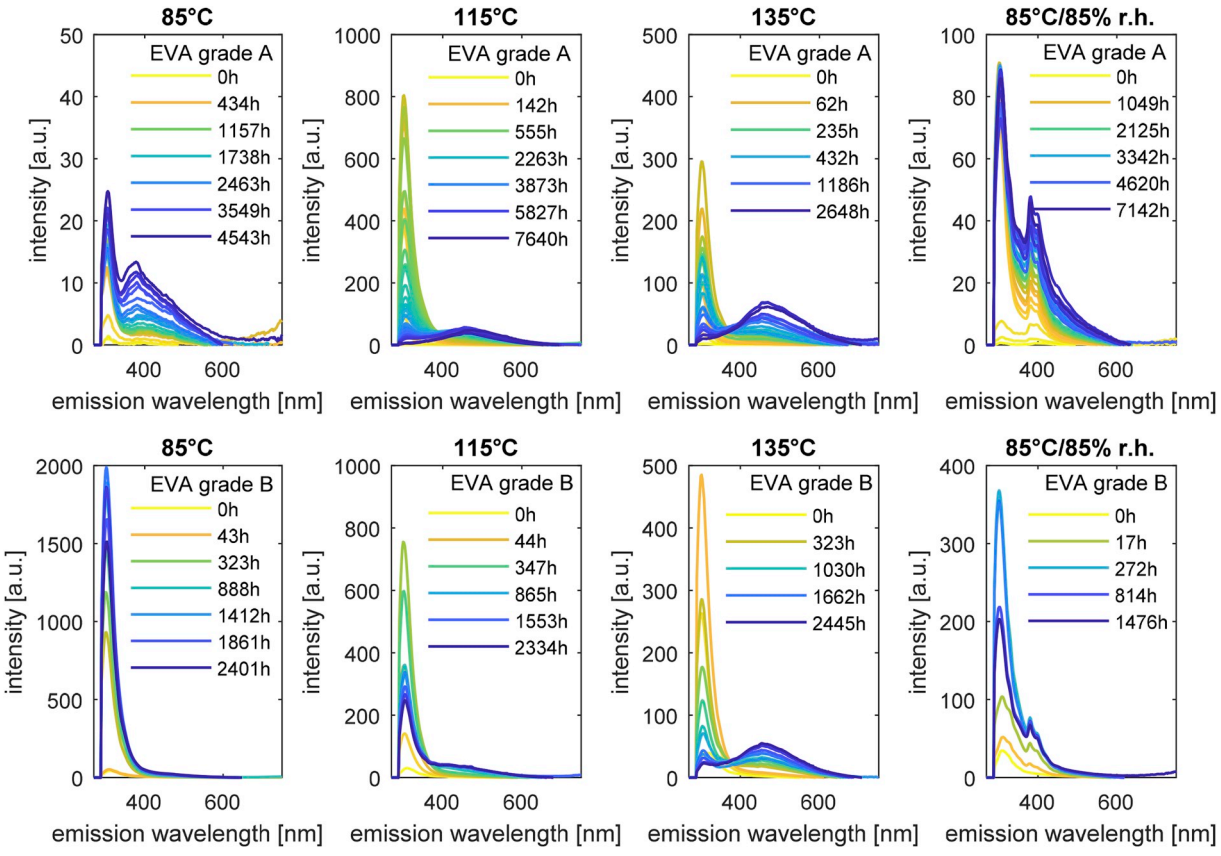

Fig. 4. 3D Photoluminescence spectra of EVA grade A (top) and EVA grade B (bottom) after 115 °C dry heat exposure excited at 280 nm employing polarizers instead of filters, i.e. including the short-wavelength (initial) photoluminescence signal.

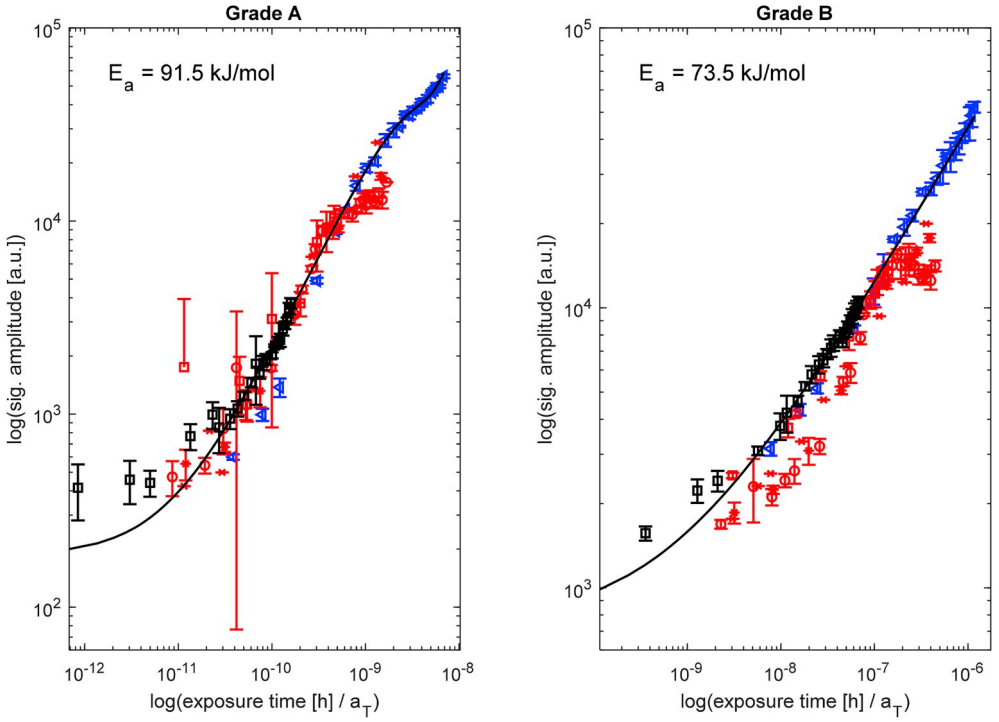

Fig. 5. TTS of DOS-photoluminescence of photoluminescence kinetics exited at 280 nm employing filters. Black (85 °C), red (115 °C) and blue (135 °C). (For interpretation of the references to color in this figure legend, the reader is referred to the Web version of this article.)

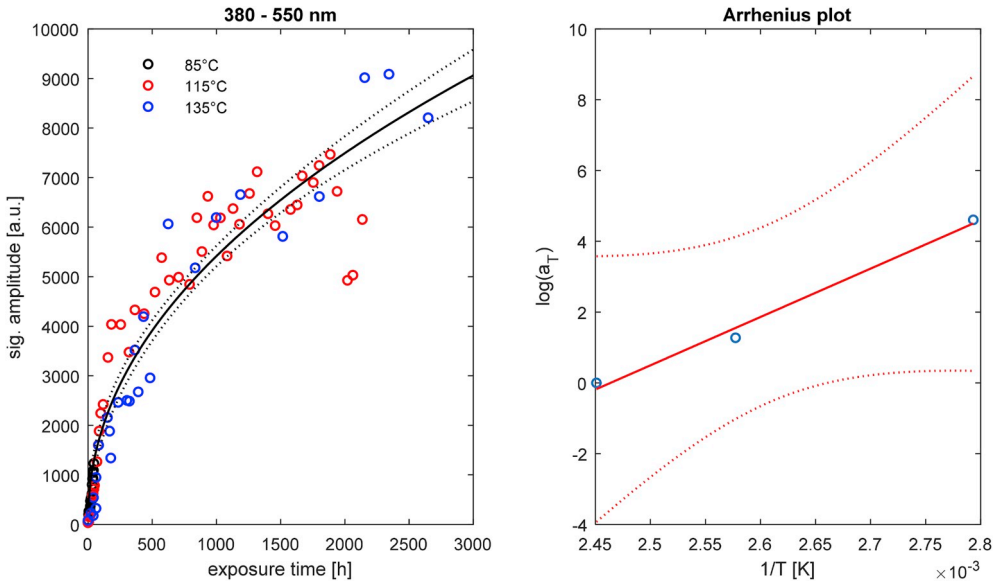

Fig. 6. TTS of DOS-photoluminescence excited at 280 nm employing polarizers instead of filters of EVA grade A from Fig. 8. Ea = 114 kJ/mol.

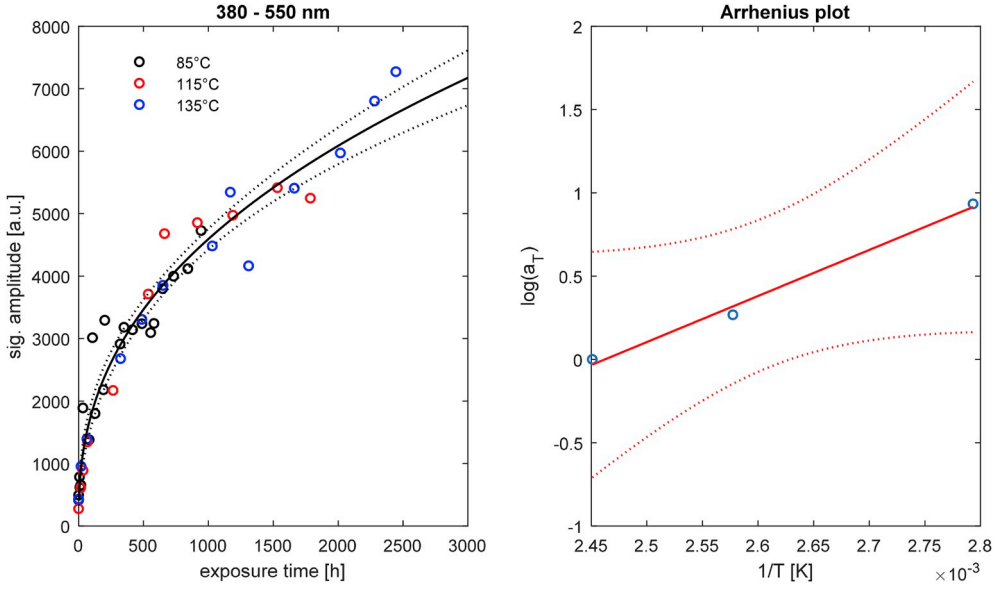

Fig. 7. TTS of DOS-photoluminescence excited at 280 nm employing polarizers instead of filters of EVA grade B from Fig. 8. Ea = 23 kJ/mol.

3.2.4. Kinetic analysis by model-testing

Fig. 8 compiles the photoluminescence kinetics extracted from the data of Fig. 4, and their corresponding fits as will be discussed in the subsequent sections.

3.2.4.1. DOS-photoluminescence. Based on the model analysis of the DOS-photoluminescence provided in our previous reports [26,27] we now perform a model-testing approach on the DOS-photoluminescence of the investigated EVA grades. As discussed in Ref. [26] the kinetics of the DOS-photoluminescence signal can be globally fit to a power-law of the form:

$$f(t,T) = a^*[k(T)(t+t_0)]^m$$

with the Arrhenius rate constant

$$k(T) = A^*\exp(-E_A/RT)$$

The resulting fits provide adjusted R^2 values better than 0.94 and are shown in the right panels of Fig. 8 with the estimated parameters complied in Table 2.

EVA grade A and EVA grade B exhibit significantly different amplitudes (a), Arrhenius pre-exponential factors (A) and apparent activation energies (E_a) for the DOS-photoluminescence kinetics. This is indicative of a different underlying degradation mechanism for the two differently stabilized EVA formulations. It also renders the absolute photoluminescence intensity of the two EVA grades incomparable.

3.2.4.2. Initial photoluminescence. As suggested above, the kinetics of the short-wavelength (initial photoluminescence) signal were fitted to a sequential model of the form:

$$f(t) = a^*\frac{\tau_1}{\tau_1-\tau_2}^*\left[\exp\left(-\frac{t}{\tau_1}\right)-\exp\left(-\frac{t}{\tau_2}\right)\right]$$

The fits are shown in Fig. 8 and the resulting estimates of the model

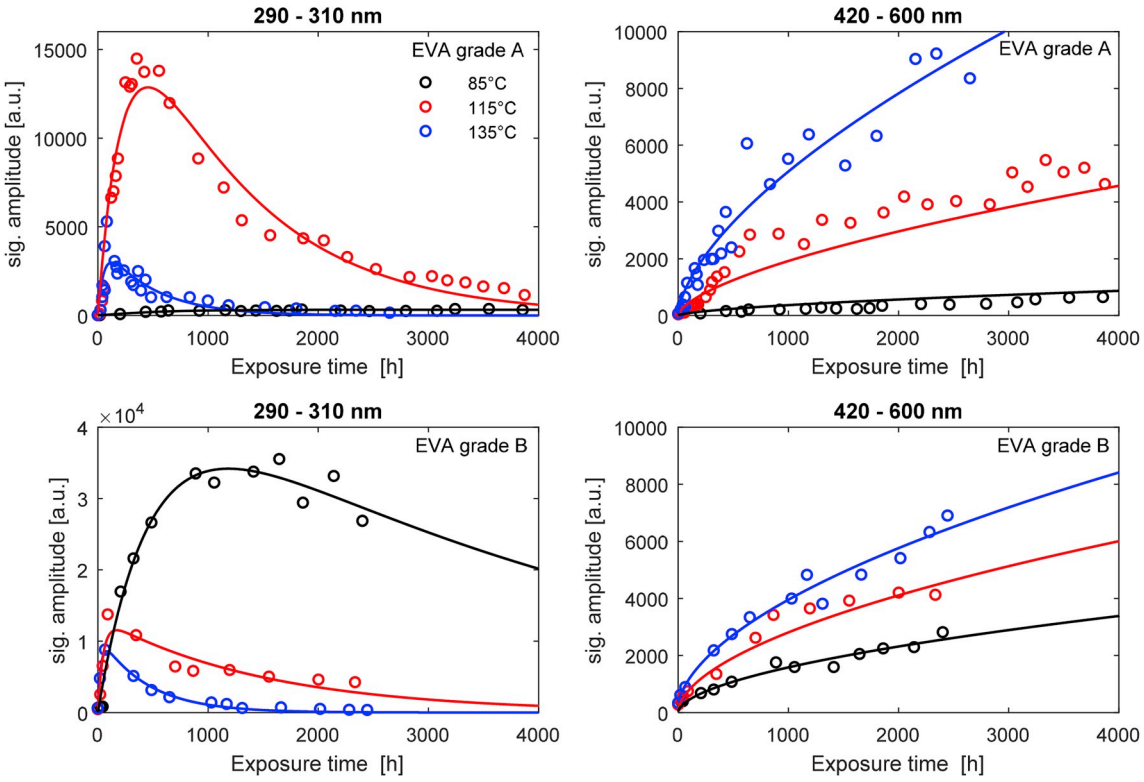

Fig. 8. Kinetics of EVA grade A (top) and EVA grade B (bottom) after 115 °C dry heat exposure for the short-wavelength (initial) signal (left) and the long-wavelength (DOS-photoluminescence) signal (right) derived from the data employing polarizers (Fig. 4).

Table 2
Parameters estimated from a global fit for the long-wavelength (380–550 nm) kinetics excited at 280 nm as shown in Fig. 8.

EVA (adjusted R^2)	Temperature [°C]	a	A	E_A	m	t_0
grade A	85	5112	1.20e10	102	0.63	0.005
0.94	115					175
	135					0.03
grade B	85	2423	346	40	0.55	40
0.97	115					24
	135					12

Table 3
Lifetimes estimated for the short-wavelength (290–310 nm) kinetics shown in Fig. 8.

EVA	Temperature [°C]	τ_1 [h]	E_a [kJ/mol]	τ_2 [h]	E_a [kJ/mol]	Adjusted R^2
grade	85	544	55	–	56	0.80
A	115	233		1074		0.95
	135	51		455		0.63
grade	85	476	71	4377	55	0.98
B	115	48		1506		0.76
	135	28		432		0.97

parameters are compiled in Table 3 . It should be emphasized, that the initial kinetics for 135 °C and 115 °C are qualitatively comparable, whereas the kinetics at 85 °C significantly differs between EVA grade A (weak mono-exponential rise) and EVA grade B (sequential kinetics). As a consequence τ_2 cannot be estimated in case of EVA grade A. This can be easily understood in the scope of a sequential reaction kinetics and indicates that at this temperature (85 °C) the initial build-up of

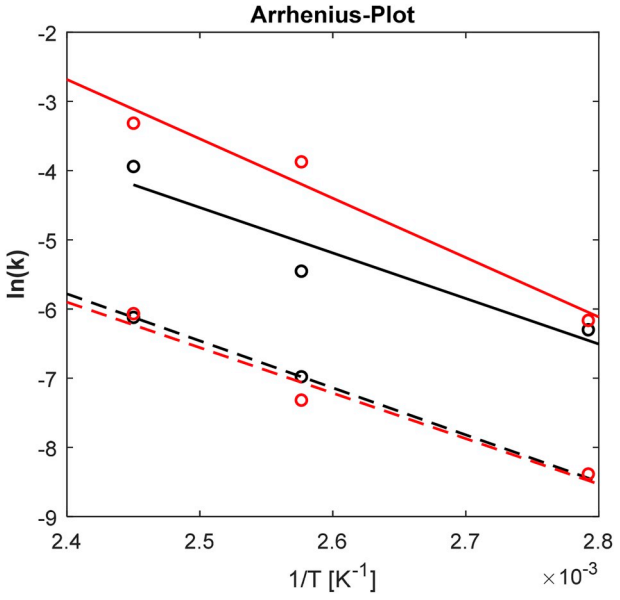

Fig. 9. Arrhenius plot of short-wavelength data from Fig. 8. Grade A (black), Grade B (red), τ_1 (solid), τ_2 (dashed). (For interpretation of the references to color in this figure legend, the reader is referred to the Web version of this article.)

Table 4
Comparison of parameters estimated for EVA grade A and EVA grade B.

Method	Property	Grade A	Grade B
Absorbance spectra	UV-absorber	+	–
Absorbance kinetics at 285 nm for 115 °C dry heat	rise/decay [h]	0.8/130	64/2078
Kinetics of initial (short-wavelength) photoluminescence, 115 °C	rise/decay [h]	233/1074	48/1506
Initial photoluminescence kinetics (polarizer, sequential model)	E_a^{rise}/E_a^{decay} [kJ/mol]	55/56	71/55
DOS-photoluminescence kinetics (filter, TTS)	E_a [kJ/mol]	92	74
DOS-photoluminescence kinetics (polarizer, TTS)	E_a [kJ/mol]	114	23
DOS-photoluminescence kinetics (polarizer, power law model)	E_a [kJ/mol]	102	41
115 °C	rise [h]	4784	765

carbonyls is significantly slower than its subsequent conversion into the DOS-luminescent state. The resulting Arrhenius-plots shown in Fig. 9 confirm the Arrhenius-type behavior of the short-wavelength photoluminescence.

4. Discussion

Summarizing the experimental results, the long-wavelength photoluminescence signal can readily be identified as the DOS-photoluminescence as suggested before, and as also observed for other polymeric materials [25]. Based on the assignment of absorbance feature iii) (Fig. 1) and comparison of absorbance and photoluminescence kinetics (Figs. 2 and 3) the initial photoluminescence signal was tentatively assigned to the direct emission of carbonyl-related states.

The fact that different kinetic parameters are obtained for EVA grade A and EVA grade B shows that additive formulations and their performance can be distinguished by comparing the kinetics of degradation-induced polymer photoluminescence. In case of the EVA grades investigated here it is known, that these are used as either front sheet (grade A, containing UV absorbing additives) or back sheet (grade B) material in photovoltaic devices (see Table 3).

Table 4 compares the properties of the two investigated EVA grades as determined from absorbance and photoluminescence measurements. Comparing the time-constants of absorbance and initial photoluminescence kinetics it is clear, that for EVA grade B (which does not contain an UV-absorbing additive) the kinetic parameters of absorbance and photoluminescence are comparable. This is not the case for EVA grade A, for which the 285 nm absorbance decays on a time-scale shorter than the rise of the initial photoluminescence signal. Instead, the time-constant of the decay of absorbance at 285 nm is identical to that of the disappearance of the UV-absorbing additive Cyasorb 531 (.i.e. 130 h), rendering the absorbance and the photoluminescence spectra of both EVA grades identical after about 400 h of exposure at 115 °C. On the other hand, the corresponding apparent activation energies of both EVA grades as estimated from the sequential model of initial photoluminescence are comparable within the estimated error range of at least ±30 kJ/mol. These apparent activation energies are in the same order of magnitude as those reported in Ref. [32] for the degradation reactions R1 and R2, suggesting H-abstraction to be the rate-limiting step for this process.

Comparing the kinetic parameters for the rise of the DOS-photoluminescence signal, major differences are found between the measurements employing filters and those employing polarizers. Based on our previous work [25–27], we will discuss the results in the scope of photoluminescence depolarization and therefore the measurements employing polarizers are better suited to gain insight into the underlying physio-chemical mechanisms. The interpretation of the resulting apparent activations energies employing filters is more complex, presumably because of the contribution of additional processes. At this stage the data available is not sufficient to provide a detailed interpretation for the apparent activation energies measured when employing filters.

The kinetic parameters for the rise of the DOS-photoluminescence obtained from the measurements employing polarizers are comparable for model-free TTS analysis and fitting to a power-law model. This fact supports the validity of both approaches, and it is therefore reasonable to average these values for the following discussion.

The average apparent activation energy estimated for the rise of DOS-photoluminescence is significantly greater for EVA grade A (108 kJ/mol) than for EVA grade B (32 kJ/mol). The former value roughly corresponds to the value reported in Ref. [32] for the degradation reactions R3/R4/R5. This might indicate that, due to the additive formulation, the degradation pathway for EVA grade A is dominated by the reactions R3 (oxidation) and R4/R5 (deacetylation, Norrish II, Norrish III), i.e. by chemical degradation, which exhibits higher apparent activation energies.

The average apparent activation energy obtained for EVA grade B is typical for secondary relaxation processes [32], indicating that physical relaxation is the rate-limiting step for EVA grade B. This means, that for grade B chemical degradation is not the rate-limiting step and the luminescent state is generated by physical relaxation, which is consistent with the finding that the absorbance and the initial photoluminescence signal rises more quickly in case of EVA grade B.

To understand the degradation behavior of two differently stabilized polymeric materials we therefore have to consider different processes: i) physical relaxation and ii) chemical degradation, as well as the cumulative history of exposure of the particular samples.

With respect to the EVA grades investigated in this study, in addition to the exposure of samples during our experiments, we have to take into account the curing process the sample went through during production. We can safely assume that both grades went through the same curing procedure, i.e. they were exposed to the same elevated temperature for the same period of time. However, because they are differently stabilized they exhibit different degrees of chemical degradation after curing. Therefore, in our experiments the EVA grade less heat-stabilized will start with a higher degree of oxidation as compared to the more heat-stabilized EVA grade.

It should also be noted that, due to the relatively rapid cooling of samples after curing, the polymeric materials are frozen in into a non-equilibrium state which very slowly relaxes towards a temperature-dependent equilibrium (physical relaxation). In our experiments this process is accelerated because we work above the melting transition of ethylene segments [15,34,40,41].

This is of importance with respect to the development of DIPL. As discussed in Ref. [25], the photoluminescent state responsible for the DOS-photoluminescence is suggested to be an interchain-state, i.e. it strongly depends on the interchain distance (it therefore exhibits a very strong temperature-dependence). Initially the mean distance between oxidation centres is relatively high, i.e. the centres exhibit the initial

photoluminescence signal (short-wavelength signal). During the process of physical relaxation the dipol-dipol interaction [42] of carbonyl groups will shorten the interchain distance. This leads to a decrease of initial photoluminescence and a corresponding increase of the DOS-photoluminescence.

Based on this model, both of the above mentioned processes (physical relaxation and chemical degradation) will contribute to the increase of DIPL. Which one is the rate-limiting step with respect to the determination of E_a depends on the exposure history and current state of the individual polymeric sample.

Before expose in our experiments the less heat-stabilized material will exhibit a high degree of degradation (oxidation), i.e. a larger relative signal of initial luminescence as compared to the more heat-stabilized sample (vide supra). During exposure at 85 °C physical relaxation (secondary relaxation) will be the dominant process (rate-limiting step) and chemical degradation will be slow, because $E_a(\textit{chemical degradation}) > E_a(\textit{physical degradation})$. Therefore, at this temperature the less heat-stabilized material will exhibit the faster rise of DIPL. At 135 °C physical relaxation is largely completed. However, because for the less heat-stabilized material the density of degradation centres is high, chemical degradation still is not rate-limiting. The overall process measured for this material will limited by secondary relaxation characterized by low E_a values.

For the more-heat stabilized sample the density of degradation centres is not sufficient for physical relaxation to decrease the mean distance of oxidation centres below the threshold where the DOS-photoluminescence signal starts to evolve. Physical relaxation therefore only contributes to the generation of DIPL once the density of degradations centres is above a certain threshold. Here chemical degradation is the rate-limiting step for the generation of the DIPL signals. The E_a measured under these circumstances is a mixture of the E_a of chemical degradation and physical relaxation.

In summary we find, that while the initial photoluminescence signal is always rate-limited by chemical degradation, the DOS-photoluminescence signal can be rate-limited by either chemical or physical relaxation.

4.1. Suggested relationship between degradation-induced polymer photoluminescence and discoloration

From the spectroscopic point of view discoloration (yellowing or browning) is a very complex phenomenon that cannot be assigned to a single chromophore species. Already Pern attributed the discoloration of EVA to the “formation of a *mixture* of chromophoric polyenes” [43].

From our point of view polyenes constitute just one of different species that can contribute to the phenomenon of discoloration. Which chromophore species contribute to discoloration in a polymeric material depends on the chemical nature of the specific polymeric material, its degradation chemistry (influenced by the additive formulation) and the applied exposure conditions. All chemical groups that contain (conjugated) double bonds, e.g. (α,β-unsaturated) carbonyls, short polyenes, amides, imines, …) can generally contribute to discoloration. This hypothesis is supported by many reports in the literature that combine investigations of discoloration of different polymeric materials with methods that identify specific chemical groups, e.g. EPR, FTIR [43–47]. Generally, a correlation is found between discoloration and the build-up of the above mentioned chemical groups.

Comparing the spectroscopic properties and suggested mechanisms for discoloration in different polymeric materials with those of the long-wavelength degradation-induced polymer photoluminescence [25], we suggest that both phenomena are governed the same underlying mechanism.

This means we suggest that discoloration is governed by the same density of states model as suggested for the long-wavelength DIPL signal. The electronic states that contribute to discoloration are then generated via inter-chain (inter-chromophore) interactions and not by a single chemical species directly. As a matter of fact, none of the above mentioned chemical groups absorb in the visible region and therefore cannot by itself cause visible discoloration. Only the electronic interaction between these groups is suggested to induce absorbance in the visible region. This idea is supported by the usually very broad and unspecific absorbance spectra of discolored samples that extend the full visible spectral region. In this study, an absorbance spectrum typical for discoloration is observed for EVA B after 1060 h of exposure to 115 °C dry heat (Fig. 1). It should be noted that under these conditions the carbonyl-related photoluminescence signal largely disappeared already (Fig. 4), which might indicate that the carbonyls generated in a first oxidation step subsequently are transformed into inter-chain states and now contribute to the density of states absorbance.

5. Conclusions

In this paper we investigate the kinetic parameters of EVA degradation of two differently stabilized EVA materials by means of degradation-induced polymer photoluminescence spectroscopy on a quantitative basis. In support of the previously discussed model of DIPL, we were able to identify the initial luminescence signal and relate it to carbonyl formation. We found that the generation of carbonyl states under dry heat exposure proceeds with an average apparent activation energy of about 60 kJ/mol for both EVA grades. In contrast, the general degradation as determined by the long-wavelength photoluminescence signal is characterized by an average apparent activation energy of about 108 kJ/mol for EVA grade A, and about 32 kJ/mol for EVA grade B.

These different apparent activation energies are explained in the scope of the density of states model of degradation-induced polymer photoluminescence considering chemical degradation and physical relaxation processes. Specifically, the photoluminescence kinetics of EVA grade A is suggested to be rate-limited by chemical degradation, whereas the kinetics for EVA grade B is, due to a higher degree of initial degradation, suggested to be rate-limited by physical relaxation. We thereby demonstrated that the complex kinetic properties, as measured by absorbance and photoluminescence spectroscopy, of differently stabilized EVA materials can be understood in the scope of the model of degradation-induced polymer photoluminescence.

Furthermore, the analytical framework described here can also be applied to other polymeric materials, enabling the application of the photoluminescence method for the development of new (organic) photovoltaic devices, the optimization and characterization of additive formulations, in industrial quality control processes or for the characterization of polymeric materials in the field.

Acknowledgements

This work was funded in the scope of the BMWi project "Langlebige Qualitätsmodule für PV-Systeme mit Speicheroption und intelligentem Energiemanagement" (LAURA, 0325716G).

References

[1] MCCd Oliveira, A.S.A. Diniz Cardoso, M.M. Viana, VdFC. Lins, The causes and effects of degradation of encapsulant ethylene vinyl acetate copolymer (EVA) in crystalline silicon photovoltaic modules: a review, Renew. Sustain. Energy Rev. 81 (2018) 2299–2317, https://doi.org/10.1016/j.rser.2017.06.039.

[2] N.D. Searle, M. McGreer, A. Zielnik, Weathering of polymeric materials, in: Encyclopedia of Polymer Science and Technology, John Wiley & Sons, Inc, Hoboken, NJ, USA, 2002, p. 161, https://doi.org/10.1002/0471440264.pst401.pub2.

[3] V. Sharma, S.S. Chandel, Performance and degradation analysis for long term reliability of solar photovoltaic systems: a review, Renew. Sustain. Energy Rev. 27 (2013) 753–767, https://doi.org/10.1016/j.rser.2013.07.046.

[4] C.J. Brabec, Organic photovoltaics: technology and market, Sol. Energy Mater. Sol. Cells 83 (2–3) (2004) 273–292, https://doi.org/10.1016/j.solmat.2004.02.030.

[5] M.C. López-Escalante, L.J. Caballero, F. Martín, M. Gabás, J.R. Ramos-Barrado, Selective emitter technology global implantation through the use of low ultraviolet

cut-off EVA, Sol. Energy Mater. Sol. Cells 159 (2017) 467–474, https://doi.org/10.1016/j.solmat.2016.09.035.
[6] M. Lämmle, H. Hernandez Gonzalez, A. Piekarczyk, L. Pita Bauermann, C. Li, M. Meir, et al., Organic PVT - a novel hybrid collector combining organic photovoltaics and polymer absorbers, in: A. Häberle (Ed.), Proceedings of EuroSun 2018, International Solar Energy Society, Freiburg, Germany, 2018, pp. 1–6, https://doi.org/10.18086/eurosun2018.02.13.
[7] A.S. Maxwell, W.R. Broughton, G.D. Dean, G.D. Sims, Review of Accelerated Ageing Methods and Lifetime Prediction Techniques for Polymeric Materials, National Physical Laboratory, Teddington, Middlesex, 2005.
[8] M. Celina, K.T. Gillen, R.A. Assink, Accelerated aging and lifetime prediction: review of non-Arrhenius behaviour due to two competing processes, Polym. Degrad. Stab. 90 (3) (2005) 395–404, https://doi.org/10.1016/j.polymdegradstab.2005.05.004.
[9] M.C. Celina, Review of polymer oxidation and its relationship with materials performance and lifetime prediction, Polym. Degrad. Stab. 98 (12) (2013) 2419–2429, https://doi.org/10.1016/j.polymdegradstab.2013.06.024.
[10] F. Pern, Factors that affect the EVA encapsulant discoloration rate upon accelerated exposure, Sol. Energy Mater. Sol. Cells 41–42 (1996) 587–615, https://doi.org/10.1016/0927-0248(95)00128-X.
[11] P. Klemchuk, M. Ezrin, G. Lavigne, W. Holley, J. Galica, S. Agro, Investigation of the degradation and stabilization of EVA-based encapsulant in field-aged solar energy modules, Polym. Degrad. Stab. 55 (3) (1997) 347–365, https://doi.org/10.1016/S0141-3910(96)00162-0.
[12] D.-W. Lee, W.-J. Cho, J.-K. Song, J.-T. Lee, C.-H. Park, K.-E. Park, et al., Degradation behaviors of EVA encapsulant and AZO films in Cu(In,Ga)Se2 photovoltaic modules under accelerated damp heat exposure, Sol. Energy Mater. Sol. Cells 136 (2015) 135–141, https://doi.org/10.1016/j.solmat.2014.12.036.
[13] C. Ferrara, D. Philipp, Why do PV modules fail? Energy Procedia 15 (2012) 379–387, https://doi.org/10.1016/j.egypro.2012.02.046.
[14] K. Agroui, A. Maallemi, M. Boumaour, G. Collins, M. Salama, Thermal stability of slow and fast cure EVA encapsulant material for photovoltaic module manufacturing process, Sol. Energy Mater. Sol. Cells 90 (15) (2006) 2509–2514, https://doi.org/10.1016/j.solmat.2006.03.023.
[15] W. Stark, M. Jaunich, Investigation of ethylene/vinyl acetate copolymer (EVA) by thermal analysis DSC and DMA, Polym. Test. 30 (2) (2011) 236–242, https://doi.org/10.1016/j.polymertesting.2010.12.003.
[16] K. Agroui, G. Collins, J. Farenc, Measurement of glass transition temperature of crosslinked EVA encapsulant by thermal analysis for photovoltaic application, Renew. Energy 43 (2012) 218–223, https://doi.org/10.1016/j.renene.2011.11.015.
[17] K. Agroui, G. Collins, Characterisation of EVA encapsulant material by thermally stimulated current technique, Sol. Energy Mater. Sol. Cells 80 (1) (2003) 33–45, https://doi.org/10.1016/S0927-0248(03)00112-0.
[18] B. Ottersböck, G. Oreski, G. Pinter, Comparison of different microclimate effects on the aging behavior of encapsulation materials used in photovoltaic modules, Polym. Degrad. Stab. 138 (2017) 182–191, https://doi.org/10.1016/j.polymdegradstab.2017.03.010.
[19] A. Charlesby, R.H. Partridge, The identification of luminescence centres in polyethylene and other polymers, Proc. R. Soc. A Math. Phys. Eng. Sci. 283 (1394) (1965) 312–328, https://doi.org/10.1098/rspa.1965.0023.
[20] I. Boustead, A. Charlesby, Identification of luminescence centres in low density polyethylene, Eur. Polym. J. 3 (3) (1967) 459–471, https://doi.org/10.1016/0014-3057(67)90014-6.
[21] N.S. Allen, J.F. McKellar, G.O. Phillips, Luminescence from thermally oxidized model amides in relation to nylon 66 degradation, J. Polym. Sci. Polym. Chem. Ed. 12 (11) (1974) 2623–2629, https://doi.org/10.1002/pol.1974.170121115.
[22] N.S. Allen, J.F. McKellar, D. Wilson, Luminescence and degradation OF nylon polymers .1. Photooxidation processes involving phosphorescent species, J. Photochem. 6 (5) (1977) 337–348.
[23] F. Pern, A. Czanderna, Characterization of ethylene vinyl acetate (EVA) encapsulant: effects of thermal processing and weathering degradation on its discoloration, Sol. Energy Mater. Sol. Cells 25 (1–2) (1992) 3–23, https://doi.org/10.1016/0927-0248(92)90013-F.
[24] A.W. Czanderna, F.J. Pern, Encapsulation of PV modules using ethylene vinyl acetate copolymer as a pottant: a critical review, Sol. Energy Mater. Sol. Cells 43 (2) (1996) 101–181, https://doi.org/10.1016/0927-0248(95)00150-6.
[25] R. Steffen, G. Wallner, J. Rekstad, B. Röder, General characteristics of photoluminescence from dry heat aged polymeric materials, Polym. Degrad. Stab. 134 (2016) 49–59, https://doi.org/10.1016/j.polymdegradstab.2016.09.032.
[26] R. Steffen, H. Setyamukti, G. Wallner, K. Geretschläger, B. Röder, Kinetics of degradation-induced polymer luminescence: polyamide under dry heat exposure, Polym. Degrad. Stab. 140 (2017) 114–125, https://doi.org/10.1016/j.polymdegradstab.2017.04.010.
[27] R. Steffen, M. Meir, J. Rekstad, B. Röder, Kinetics of degradation-induced polymer luminescence: a polyphenylene sulfide/elastomer blend under dry heat exposure, Polymer (2017), https://doi.org/10.1016/j.polymer.2017.12.045.
[28] J.C. Schlothauer, K. Grabmayer, I. Hintersteiner, G.M. Wallner, B. Röder, Non-destructive 2D-luminescence detection of EVA in aged PV modules: correlation to calorimetric properties, additive distribution and a clue to aging parameters, Sol. Energy Mater. Sol. Cells 159 (2017) 307–317, https://doi.org/10.1016/j.solmat.2016.09.011.
[29] J.C. Schlothauer, C. Peter, C. Hirschl, G. Oreski, B. Röder, Non-destructive monitoring of ethylene vinyl acetate crosslinking in PV-modules by luminescence spectroscopy, J. Polym. Res. 24 (12) (2017) 203, https://doi.org/10.1007/s10965-017-1409-y.
[30] J.C. Schlothauer, R.M. Ralaiarisoa, A. Morlier, M. Koentges, B. Roeder, Determination of the cross-linking degree of commercial ethylene-vinyl-acetate polymer by luminescence spectroscopy, J. Polym. Res. 21 (5) (2014), https://doi.org/10.1007/s10965-014-0457-9.
[31] A. Morlier, M. Köntges, S. Blankemeyer, I. Kunze, Contact-free determination of ethylene vinyl acetate crosslinking in PV modules with fluorescence emission, Energy Procedia 55 (2014) 348–355, https://doi.org/10.1016/j.egypro.2014.08.101.
[32] M. Gagliardi, P. Lenarda, M. Paggi, A reaction-diffusion formulation to simulate EVA polymer degradation in environmental and accelerated ageing conditions, Sol. Energy Mater. Sol. Cells 164 (2017) 93–106, https://doi.org/10.1016/j.solmat.2017.02.014.
[33] X.E. Cai, H. Shen, Apparent activation energies of the non-isothermal degradation of EVA copolymer, J. Therm. Anal. 55 (1) (1999) 67–76, https://doi.org/10.1023/A:1010175904064.
[34] A. Badiee, I.A. Ashcroft, R.D. Wildman, The thermo-mechanical degradation of ethylene vinyl acetate used as a solar panel adhesive and encapsulant, Int. J. Adhesion Adhes. 68 (2016) 212–218, https://doi.org/10.1016/j.ijadhadh.2016.03.008.
[35] Talrose V, Yermakov AN, Usov AA, Goncharova AA, Leskin AN, Messineva NA et al. UV/Visible spectra. In: Linstrom P, editor. NIST Chemistry WebBook, NIST Standard Reference Database vol. 69: National Institute of Standards and Technology. doi:10.18434/T4D303.
[36] H. Kaczmarek, A. Kamińska, A. van Herk, Photooxidative degradation of poly(alkyl methacrylate)s, Eur. Polym. J. 36 (4) (2000) 767–777, https://doi.org/10.1016/S0014-3057(99)00125-1.
[37] M. Gardette, A. Perthue, J.-L. Gardette, T. Janecska, E. Földes, B. Pukánszky, et al., Photo- and thermal-oxidation of polyethylene: comparison of mechanisms and influence of unsaturation content, Polym. Degrad. Stab. 98 (11) (2013) 2383–2390, https://doi.org/10.1016/j.polymdegradstab.2013.07.017.
[38] M. Rodríguez-Vázquez, C.M. Liauw, N.S. Allen, M. Edge, E. Fontan, Degradation and stabilisation of poly(ethylene-stat-vinyl acetate): 1 – spectroscopic and rheological examination of thermal and thermo-oxidative degradation mechanisms, Polym. Degrad. Stab. 91 (1) (2006) 154–164, https://doi.org/10.1016/j.polymdegradstab.2005.04.034.
[39] J. Dealy, D. Plazek, Time-temperature superposition - a users guide, Rheol. Bull. 78 (2) (2009) 16–31.
[40] C. Motta, The effect of copolymerization on transition temperatures of polymeric materials, J. Therm. Anal. 49 (1) (1997) 461–464, https://doi.org/10.1007/BF01987471.
[41] H.-Y. Li, L.-E. Perret-Aebi, R. Théron, C. Ballif, Y. Luo, R.F.M. Lange, Optical transmission as a fast and non-destructive tool for determination of ethylene-co-vinyl acetate curing state in photovoltaic modules, Prog. Photovolt. Res. Appl. 21 (2) (2013) 187–194, https://doi.org/10.1002/pip.1175.
[42] F.H. Allen, C.A. Baalham, J.P.M. Lommerse, P.R. Raithby, Carbonyl–carbonyl interactions can be competitive with hydrogen bonds, Acta. Crystallogr. B Struct. Sci. 54 (3) (1998) 320–329, https://doi.org/10.1107/S0108768198001463.
[43] F.J. Pern, Polymer encapsulants characterized by fluorescence analysis before and after degradation, in: Photovoltaic Specialists Conference, Conference Record of the Twenty Third IEEE, 1993, pp. 1113–1118, https://doi.org/10.1109/PVSC.1993.346968.
[44] N.S. Allen, M. Edge, M. Rodriguez, C.M. Liauw, E. Fontan, Aspects of the thermal oxidation of ethylene vinyl acetate copolymer, Polym. Degrad. Stab. 68 (3) (2000) 363–371, https://doi.org/10.1016/S0141-3910(00)00020-3.
[45] N.S. Allen, M. Edge, A. Wilkinson, C.M. Liauw, D. Mourelatou, J. Barrio, et al., Degradation and stabilisation of styrene–ethylene–butadiene–styrene (SEBS) block copolymer, Polym. Degrad. Stab. 71 (1) (2000) 113–122, https://doi.org/10.1016/S0141-3910(00)00162-2.
[46] N. Rajagopalan, A.S. Khanna, Effect of methyltrimethoxy silane modification on yellowing of epoxy coating on UV (B) exposure, J. Coatings 2014 (4) (2014) 1–7, https://doi.org/10.1155/2014/515470.
[47] A.E. Krauklis, A.T. Echtermeyer, Mechanism of yellowing: carbonyl Formation during hygrothermal aging in a common amine epoxy, Polymers 10 (9) (2018), https://doi.org/10.3390/polym10091017.